Novel Bimolecular Reactions between NH_3 and HNO_3 in the Gas Phase

R. N. Musin

Institute of Chemical Kinetics and Combustion, Russian Academy of Sciences, Novosibirsk, 630090, Russia

M. C. Lin*

Department of Chemistry, Emory University, Atlanta, Georgia 30322

Received: November 10, 1997; In Final Form: January 8, 1998

High-level molecular orbital calculations have been performed in the framework of the G2M method to explore the reactivity between NH_3 and HNO_3, key molecular reactants in ammonium nitrate and ammonium nitramide systems. Two nonionic molecular reaction channels have been identified with a similar reaction barrier, 46 kcal/mol. One channel occurring via a four-member-ring transition state produces $H_2NNO_2 + H_2O$ (1), and the other, taking place via a five-member-ring transition state, yields $H_2NONO + H_2O$ (2). A transition-state theory calculation employing the predicted energies and molecular parameters gave rise to the rate constants $k_1 = 0.81T^{3.47}e^{-21670/T}$ and $k_2 = 23.2T^{3.50}e^{-22610/T}$ for the temperature range 300−3000 K in units of $cm^3/(mol\cdot s)$. In addition to the reactants, products, and transition states associated with the two reaction channels, several local minima (or molecular complexes) and secondary reaction products derived from the structural rearrangement of some of the molecular complexes, such as H_3NO and H_2NOH, have been identified and their energies calculated at the G2M level of theory.

I. Introduction

Ammonium salts are unstable in their ionic forms at elevated temperatures; they typically sublime to yield ammonia and acids under low-pressure conditions. For ammonium nitrate, NH_3 and HNO_3 are the low-pressure sublimation products. Under atmospheric or higher pressure conditions, however, NH_4NO_3 melts near 520 K to produce primarily N_2O and H_2O via ionic reactions, presumably involving NO_2^+ and NH_3.[1,2]

In our present series of studies on the mechanisms of reactions involving H/N/O-containing species in conjunction with their potential applications to propulsion and the reduction of NO_x with NH_3,[3−17] we have investigated the interaction of NH_3 and HNO_3, over the temperature range 700−1000 K.[18]

The $NH_3 + HNO_3$ reaction above 800 K can be quantitatively characterized by a radical chain process initiated by the decomposition of HNO_3, $HNO_3 + M \rightarrow OH + NO_2 + M$, followed by $OH + NH_3$ and the reactions of NH_2 with NO_x, leading to the formation of N_2 and N_2O. At temperatures below 800 K, at which the rate of the HNO_3 decomposition reaction becomes slower, the same radical mechanism was found to be inadequate for the prediction of the NH_3 decay rate and the rates of N_2O and H_2O formation.[18]

To search for the processes responsible for the observed "enhanced" rates of the reaction, we have carried out a comprehensive ab initio molecular orbital (MO) theory study of the bimolecular reaction of NH_3 and HNO_3 focusing on the direct interaction of the nucleophilic N atom in NH_3 with the electrophilic N atom in HNO_3. The investigation reveals for the first time two reaction paths leading to the formation of highly reactive molecular intermediates, H_2NNO_2 and H_2NONO. These reactive species, whose stabilities have been calculated in our previous study on the $NH_2 + NO_2$ reaction,[7] may be responsible for the enhanced rate of the $NH_3 + HNO_3$ reaction in the low-temperature regime ($T \leq 800$ K), particularly under high-pressure conditions. The results of the ab initio MO calculation and the predicted rate constants for these novel redox processes by the transition-state theory (TST) are reported herein.

II. Computation Methods

The potential energy surface for the reaction of ammonia with nitric acid was studied in the framework of the ab initio G2M method,[6] which is a modification of the Gaussian-2 (G2) methodology, developed by Pople and co-workers.[19] It has been shown earlier that various schemes of the G2M approach enable accurate predictions of the energetics of molecular systems with closed and open shells containing up to six to eight heavy atoms.[6,20,21] In the present paper, we have employed the G2M-(RCC,MP2) scheme of the G2M method, which gives an average absolute deviation of 1.15 kcal/mol of calculated atomization energies from experiments for 32 first-row compounds tested by the original G2 method[19] (in the case of triple-ζ basis set 6-311G(d,p) with 2p and 3d polarization functions). This approach includes a series of MPn (Møller−Plessett perturbation method of the nth order)[22] and RCCSD(T) (restricted single- and double-excitation coupled cluster method)[23] calculations to improve the MP4 base energy $E_{bas} = E$[PMP4/6-311G(d,p)] with the correction for electron correlation,

$$\Delta E(\text{RCC}) = E[\text{RCCSD(T)/6-311G(d,p)}] - E_{bas}$$

the correction for basis set expansion,

$$\Delta E(+3\text{df2p}) = E[\text{PMP2/6-311+G(3df,2p)}] - E[\text{PMP2/6-311G(d,p)}]$$

and the empirical "higher level correction" given in hartrees,

$$\Delta E(\text{HLC,RCC5}) = -0.00525n_\beta - 0.00019n_\alpha$$

based on the number of paired and unpaired electrons. Here,

* Corresponding author. E-mail address: chemmcl@emory.edu.

S1089-5639(98)00137-6 CCC: $15.00
Published on Web 02/12/1998

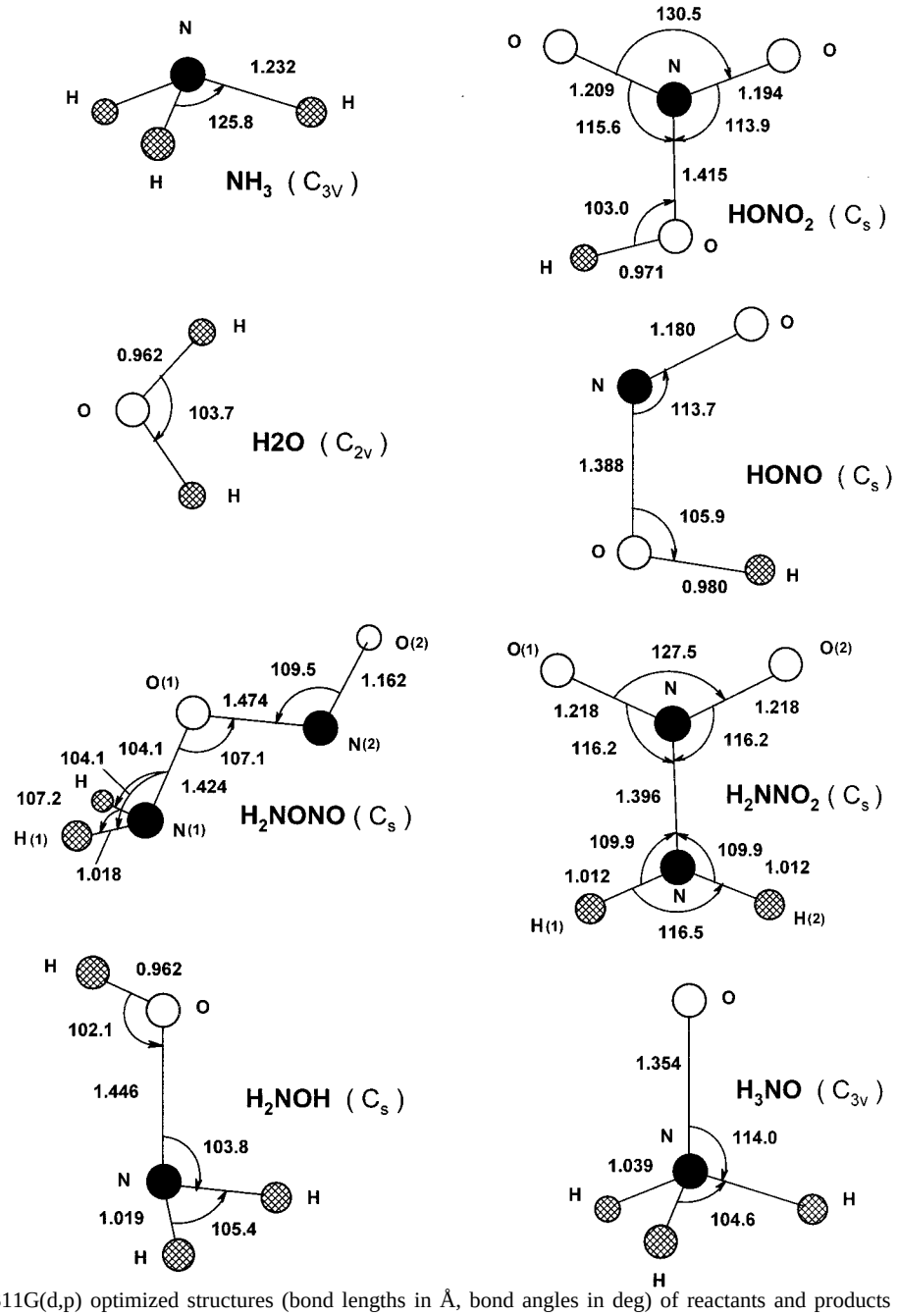

Figure 1. B3LYP/6-311G(d,p) optimized structures (bond lengths in Å, bond angles in deg) of reactants and products involved in the $NH_3 + HNO_3$ reaction.

TABLE 1: Total Energies and ZPE (in hartrees) of Reactants and the Relative Energies (in kcal/mol, ZPE Included) of Intermediates LM*n* ($n = 1-4$), Transition States TS*n* ($n = 1-4$), and Products for the $NH_3 + HONO_2$ Reaction, Calculated by B3LYP, MP2, RCCSD(T), and G2M Methods

species	ZPE	B3LYP/ 6-311G(d,p)	MP2/ 6-311G(d,p)	MP2/6-311 +G(3df,2p)	RCCSD(T)/ 6-311G(d,p)	G2M (RCC,MP2)
			Reactants			
$NH_3 + HONO_2$	0.060 766	−337.482 643	−336.660 643	−336.881 027	−336.704 585	−337.012 009
			Intermediates and Transition States			
TS1	36.91	37.48	38.54	37.74	46.45	45.66
TS2	35.65	57.68	50.51	51.30	45.18	45.96
LM1	40.36	−20.80	−21.22	−20.33	−20.45	−19.56
LM2	38.14	6.63	7.86	9.00	1.46	2.60
TS3	39.12	36.82	43.79	41.51	37.09	34.80
LM3	39.34	36.95	44.19	41.82	34.50	35.12
LM4	40.14	3.32	6.64	10.81	0.29	4.46
TS4	39.35	6.97	9.80	13.62	3.41	7.23
			Products			
$H_3NO + HONO$	37.77	29.50	49.20	45.32	42.05	38.16
$H_2NOH+HONO$	37.74	20.27	22.96	24.80	15.81	17.66
$H_2NONO+H_2O$	38.12	11.49	14.92	14.55	8.11	7.74
$H_2NNO_2 + H_2O$	39.87	−11.22	−11.11	−12.45	−10.69	−12.03

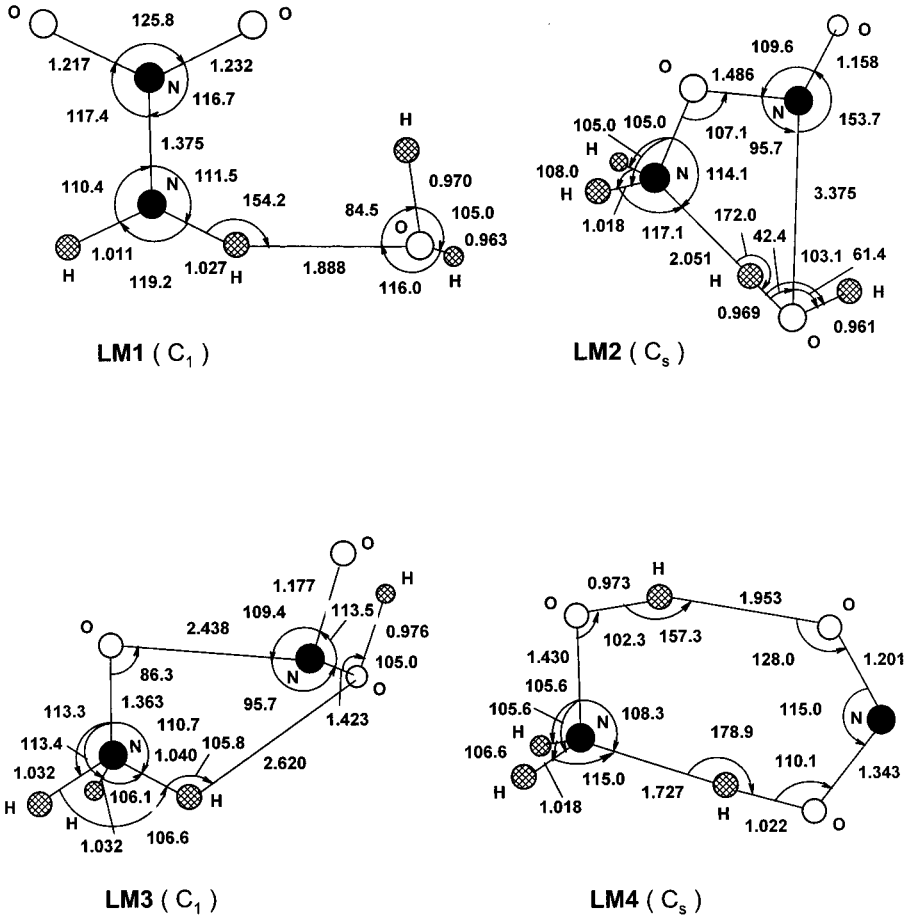

Figure 2. B3LYP/6-311G(d,p) optimized structures (bond lengths in Å, angles in deg) of intermediates of the $NH_3 + HNO_3$ reaction.

TABLE 2: Optimized Geometries (in Å and deg) for H_2NNO_2 and NH_2ONO Species, Calculated by Using HF, MP2, MCSCF, and B3LYP Methods: Comparison with Experimental Data

geometr. parameters	HF/ 6-31G(d)[a]	MP2/ 6-311G(d,p)[b]	MCSCF/ 4-31G[c]	B3LYP/ 6-311G(d,p)[d]	expt[e]
		H_2NNO_2			
N(1)N(2)	1.356	1.403	1.418	1.396	1.381
O(1)N(2)	1.191	1.221	1.227	1.218	1.232
N(1)H(1)	0.998	1.013	0.991	1.012	1.007
∠HNH	116.8	114.0	123.3	116.5	120.9
∠ONO	127.0	127.8	126.6	127.5	132.7
∠N(2)N(1)H	110.5	108.2	113.5	109.9	132.7
∠N(1)N(2)O	116.5	116.1	116.7	116.2	113.6
∠O(2)N(2)O(1)N(1)	177.6	179.4	178.1	176.5	
∠H(1)N(1)N(2)O(1)	25.6	28.3	16.8	27.0	
		NH_2ONO			
N(1)O(1)	1.393	1.421	1.413	1.424	
O(1)N(2)	1.356	1.455	1.675	1.474	
N(2)O(2)	1.153	1.175	1.164	1.162	
N(1)H(1)	1.002	1.017	0.996	1.018	
∠H(1)N(1)O(1)	104.5	103.9	108.1	104.1	
∠N(1)O(1)N(2)	108.7	106.2	105.5	107.1	
∠H(1)N(1)H(2)		106.8	114.3	107.2	
∠H(1)N(1)O(1)N(2)	123.5	124.2	117.9	124.0	
∠O(2)N(2)O(1)N(2)	180.0	180.0	180.0	180.0	

[a] Reference 28. [b] Reference 7. [c] Reference 29. [d] Present work. [e] Reference 30.

PMP*n* stands for the spin-projected PUMP*n* energies for open shell systems and RMP*n* energies for closed shell systems, and n_α and n_β are the number of α and β valence electrons ($n_\alpha \geq n_\beta$), respectively. The ZPE (zero-point energy)-corrected total energy of molecular systems in this scheme is expressed as follows:

$$E[\mathrm{G2M(RCC,MP2)}] = E_{\mathrm{bas}} + \Delta E(\mathrm{RCC}) + \Delta E(+3\mathrm{df2p}) + \Delta E(\mathrm{HLC,RCC5}) + \mathrm{ZPE[B3LYP/6\text{-}311G(d,p)]}$$

The largest calculation in this case is RCCSD(T)/6-311G-(d,p).

The structural parameters of the reactants NH_3 and HNO_3, various intermediates, transition states, and products H_2O, H_2-NOH, HONO, H_2NNO_2, H_2NONO, and H_3NO have been optimized using Becke's three-parameter nonlocal exchange functional[24] with the nonlocal correlation functional of Lee, Yang, and Parr[25] (B3LYP approach) with the 6-311G(d,p) basis set.[22] The same (B3LYP/6-311G(d,p)) method was used for calculation of vibrational frequencies which are necessary for the determination of the nature of different stationary points, as well as obtaining the accurate values of ZPE correction (without scaling) for these points and rate constant calculations. The stationary points (transition states and adjacent local minima) along the reaction paths have been connected by using the intrinsic reaction coordinate (IRC) calculations[26] at the B3LYP/6-311G(d,p) level. All the calculations have been performed by using the GAUSSIAN-94[27] program.

III. Results and Discussion

A. Molecular and Transition-State Structures. The total energy of the reactants and the relative energies of the transition states, long-lived intermediates (or local minima), and separated products calculated at various levels of theory are summarized in Table 1. The vibrational frequencies and geometries of individual species calculated at the B3LYP/6-311G(d,p) level of theory are presented in Table 4 and Figures 1−3, respectively. The structures and energies of the key products, NH_2NO_2 and NH_2ONO, as alluded to earlier, have been calculated previously in this laboratory by Mebel et al. in conjunction with the $NH_2 + NO_2$ reaction at the MP2/6-311G(d,p) level of theory.[7] The

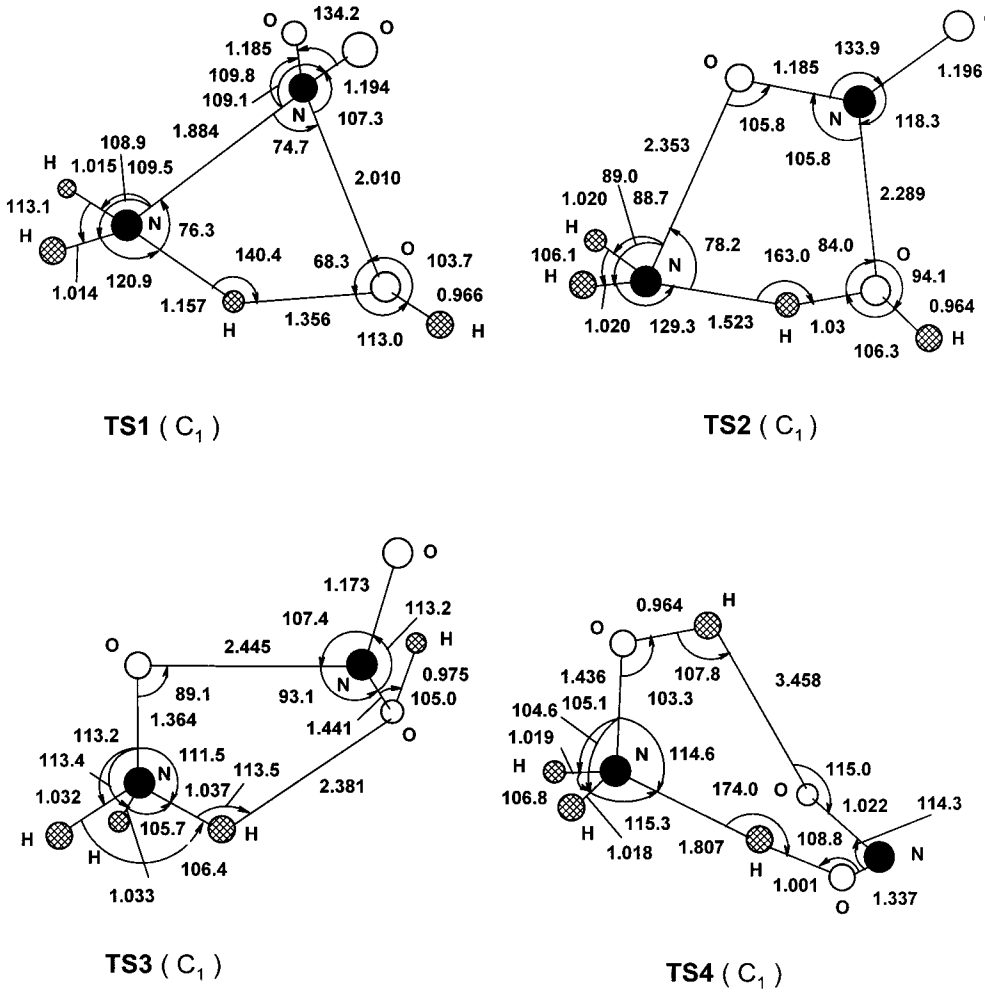

Figure 3. B3LYP/6-311G(d,p) optimized structures (bond lengths in Å, angles in deg) of transition states of the $NH_3 + HNO_3$ reaction.

TABLE 3: Optimized Geometries (in Å and deg) for H_2NOH and H_3NO Species, Calculated by Using HF, MP2, and B3LYP Methods

geometr. parameters	HF/6-31G(d)[a]	MP2/6-31G(d)[a]	MP2/6-311G(d,p)[b]	MP2/TZ2P[b]	MP2/QZ3P[b]	B3LYP/6-311G(d,p)[c]	expt[b]
			H_2NOH				
NO	1.403	1.451	1.449	1.446	1.443	1.446	1.453
OH(1)	0.946	0.971	0.964	0.960	0.958	0.962	0.962
NH(2)	1.002	1.021	1.016	1.012	1.011	1.019	1.016
∠H(1)ON	104.2	101.3	101.2	101.7	102.0	102.1	101.4
∠H(2)NO	104.8	102.9	103.0	103.5	103.8	103.8	103.2
∠H(2)NH(3)			105.0	106.0	106.2	105.4	107.1
∠θ			68.3	67.2	66.7	66.8	67.3
∠H(1)ONH(2)	124.0	125.3				125.0	
			H_3NO				
NO	1.376	1.421				1.354	
NH	1.010	1.036				1.039	
∠HNO	111.7	113.2				114.0	

[a] Reference 32. [b] Reference 31. [c] Present work.

H_2NNO_2 product has C_s symmetry. The NNO_2 fragment is nearly coplanar, while the H_2NN fragment is slightly pyramidal. The C_s mirror plane containing the N−N bond is perpendicular to the NNO_2 plane. The symmetry of the H_2NONO product is also C_s. The two hydrogen atoms of the pyramidal H_2NO group are reflected by the mirror plane involving the planar NONO chain. As has been shown earlier,[7] four different isomers of H_2NONO ((1) H-cis/NONO-cis; (2) H-cis/NONO-trans; (3) H-trans/NONO-cis; (4) H-trans/NONO-trans) can be formed in the $H_2N + ONO$ reaction depending on the approaching angle of the reactants. As follows from our IRC calculation, only the isomer H-trans/NONO-trans of H_2NONO can be obtained directly in the case of the $NH_3 + HNO_3$ reaction under consideration. According to Table 2, the values of geometric parameters (bond lengths and angles) of the H_2NNO_2 and H_2NONO species optimized by us at the B3LYP/6-311G(d,p) level of theory are in good accord with the values calculated earlier[7,28,29] in the framework of the HF/6-31G(d), MP2/6-311G(d,p), and MCSCF/4-31G methods, and with the data of experimental measurements.[30] Note that in the case of the O(1)N(2) bond length our B3LYP/6-311G(d,p) result differs by 0.201 Å from that of MCSCF/4-31G.[29] As pointed out by Saxon and Yoshimine,[29] it is possible that the length of the O(1)N(2) bond is overestimated by the MCSCF/4-31G approach.

TABLE 4: Moments of Inertia (in 10^{-40} g·cm^2) and Vibrational Frequencies for Reactants, Products, Intermediates, and Transition States of the Reaction $NH_3 + O_2NOH$, Calculated at the B3LYP/6-311G(d,p) Level

species	I_i	ν_j (cm^{-1})
NH_3	2.9	1068.6, 1681.4, 1681.7, 3463.7, 3583.1, 3583.3
	2.9	
	4.5	
$HONO_2$	64.9	484.0, 588.8, 653.8, 775.4, 910.5, 1328.0, 1358.8, 1778.8, 3733.3
	70.2	
	135.1	
TS1	152.2	1165.2i, 249.7, 286.2, 323.6, 342.6, 372.5, 585.0, 631.1, 668.4, 726.1, 779.5, 805.2, 953.1, 1317.9, 1501.9, 1666.5, 1783.6, 1882.6, 3506.8,
	187.7	3632.5, 3803.2
	204.2	
TS2	124.4	155.2i, 95.1, 229.7, 259.4, 276.1, 319.7, 366.3, 447.2, 488.7, 562.0, 616.3, 732.5, 986.4, 1308.3, 1541.0, 1676.3, 1769.4, 2417.9, 3456.6,
	259.0	3553.1, 3835.3
	374.5	
LM1	74.9	79.7, 160.1, 205.9, 245.6, 317.5, 519.0, 576.6, 608.0, 691.7, 780.2, 831.4, 1038.4, 1285.2, 1393.9, 1635.5, 1642.4, 1684.6, 3320.9, 3625.5,
	313.5	3720.4, 3872.8
	379.7	
LM2	138.5	18.7, 59.5, 124.8, 165.7, 194.9, 268.2, 304.2, 411.5, 486.5, 604.0, 773.4, 1015.6, 1168.5, 1331.1, 1665.4, 1673.7, 1825.2, 3459.4, 3548.0,
	326.4	3708.3, 3874.7
	460.0	
LM3	95.7	32.2, 141.7, 146.2, 174.7, 212.6, 307.0, 563.3, 641.2, 832.2, 964.3, 1174.7, 1178.8, 1314.5, 1545.4, 1631.8, 1638.2, 1723.6, 3159.7, 3242.2,
	291.4	3261.9, 3635.4
	342.0	
LM4	96.2	71.1, 180.3, 205.1, 217.5, 275.8, 401.4, 595.1, 738.9, 979.1, 1038.6, 1126.2, 1180.8, 1315.6, 1502.0, 1516.3, 1649.7, 1669.8, 2797.5, 3448.3,
	301.4	3520.1, 3651.5
	393.1	
TS3	95.0	125.1i, 77.9, 144.7, 154.4, 210.0, 295.9, 524.9, 634.7, 810.9, 961.7, 1173.6, 1179.5, 1296.4, 1560.6, 1622.1, 1635.3, 1737.7, 3197.5, 3244.8,
	285.4	3259.0, 3644.9
	343.7	
TS4	89.3	68.7i, 55.6, 90.9, 188.8, 228.9, 247.3, 439.5, 698.7, 965.5, 981.3, 1061.8, 1181.2, 1323.3, 1435.6, 1463.3, 1662.5, 1677.5, 3047.9, 3447.6,
	408.7	3525.3, 3802.3
	451.8	
H_3NO	4.5	931.3, 1176.6, 1176.6, 1593.5, 1624.8, 1624.8, 3123.5, 3123.5, 3153.2
	31.2	
	31.2	
HONO	10.0	638.3, 718.2, 892.6, 1337.9, 1720.6, 3582.3
	63.7	
	73.7	
H_2NOH	4.4	475.6, 921.2, 1144.4, 1320.4, 1373.0, 1652.5, 3406.0, 3506.2, 3711.2
	33.1	
	33.2	
H_2NONO	15.9	190.9, 259.2, 376.9, 499.2, 760.5, 1009.0, 1168.1, 1336.8, 1666.3, 1804.9, 3451.6, 3539.3
	173.1	
	184.5	
H_2NNO_2	66.8	427.4, 572.7, 627.6, 729.4, 810.0, 1014.5, 1239.6, 1386.8, 1612.1, 1687.2, 3525.9, 3658.3
	71.1	
	136.9	
H_2O	1.1	1639.6, 3810.0, 3906.2
	1.9	
	3.0	

The structure of **TS1** leading to the formation of H_2NNO_2 is substantially tighter than that of **TS2**, which gives rise to its less stable isomer H_2NONO, although their energies are effectively the same as discussed below.

The structures of HONO, H_3NO, and its structural isomer, H_2NOH, are shown in Figure 1. The optimized geometries of the H_2NOH and H_3NO products are presented in Table 3. One can see that the results of our B3LYP/6-311G(d,p) optimization are similar to those obtained by HF/6-31G(d) and MP2 (with different basis sets) methods as well as to experimental data.[31,32] Note that the $NH_3 + HNO_3$ reaction leads to the formation of *trans*-H_2NOH and planar *cis*-HONO products of C_s symmetry. The plane of symmetry of hydroxylamine coincides with the N−OH (hydroxyl group) plane. The optimized geometries of the stable intermediates (local minima **LM1** and **LM2**) and transition states (**TS1**−**TS4**) are shown in Figures 2 and 3, respectively. All intermediates of the reaction under consideration are found to be typically weak molecular complexes (as seen from the analysis of structural peculiarities and characters of chemical bonds of these species) with distinct hydrogen bonds.

One of the most interesting findings from the present study is the facile conversion of the $H_2NONO-H_2O$ molecular complex, **LM2** (which is about 5 kcal/mol more stable than its separated products, H_2NONO and H_2O), to H_3NO and HONO with only a 32 kcal/mol barrier, as will be discussed later.

B. Potential Energy Surface. A schematic energy diagram for the potential energy surface of the $NH_3 + HNO_3$ reaction, calculated at the G2M(RCC,MP2) level of the theory, is presented in Figure 4. The reaction takes place via two energetically comparable channels I and II as alluded to above. The first exothermic channel produces H_2NNO_2 species via transition state **TS1** with a predicted 45.7 kcal/mol activation barrier with the formation of the intermediate molecular complex **LM1**, which has a 7.6 kcal/mol potential well. The second channel is slightly endothermic and leads to the formation of H_2NONO via transition state **TS2** and molecular complex **LM2**. In this case, the values of the activation barrier and potential

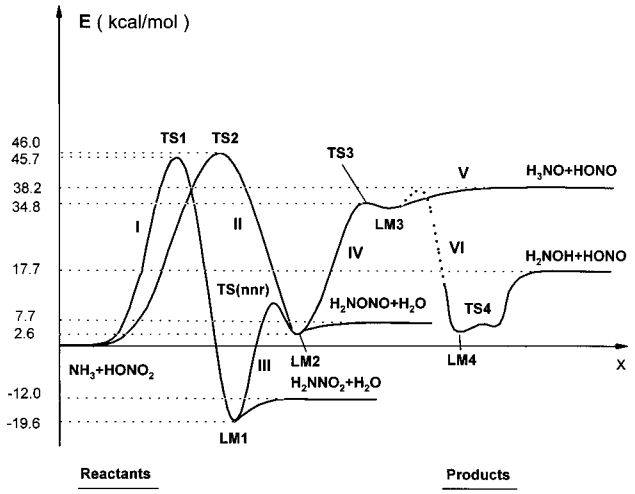

Figure 4. A schematic energy diagram for the potential energy surface of the $NH_3 + HNO_3$ reaction calculated in the framework of the G2M-(RCC,MP2)//B3LYP/6-311G(d,p) approach.

well are 46.0 and 5.1 kcal/mol, respectively. The presence of these shallow wells on the potential energy surface is expected to have a negligible effect on the formation of the energetic nitramide products in view of the great excess of energy they possess after their passage over the transition states. We have not investigated the pathway III connecting two stationary points **LM1** and **LM2** on the potential surface of the $NH_3 + HNO_3$ reaction. The existence of this channel corresponding to the nitro−nitrite rearrangement of H_2NNO_2 into H_2NONO via transition state **TS(nnr)** was studied in detail theoretically earlier.[7] For instance, calculations in the framework of the Gaussian-2 (G2) method, carried out by Mebel with coauthors,[7] show that the barrier for such structural rearrangement at the transition state **TS(nnr)** is 31.2 kcal/mol with respect to the energy level of H_2NNO_2, i.e., 11.6 kcal/mol higher than the level of the reactants $NH_3 + HNO_3$.

It has been found from our IRC calculations that there are two subsequent reaction channels IV → V and IV → VI, which begin from intermediate **LM2** and lead to the formation of H_3NO, H_2NOH, and HONO products via transition state **TS3** and local minima **LM3**.

According to the result of our IRC calculations, **LM2**, the complex of H_2NONO and H_2O, can undergo structural rearrangement via **TS3** and **LM3** (see Figure 1), producing H_3NO + HONO by direct dissociation as well as the more stable products NH_2OH + HONO, followed by the rotation of HONO in **LM3** and the exchange of H atoms as clearly indicated by the structures of **LM4** and **TS4**. The negligibly small barrier associated with the rotation of HONO at **LM3** was not calculated.

Theoretically, the unimolecular isomerization of H_3NO to H_2NOH has been investigated by many groups.[31−34] The barrier for the isomerization reaction was calculated to be 25.0 kcal/mol at the G2M(RCC,MP2) level of theory, agreeing closely with the results of previous calculations.[31,32] The isomerization reaction in the present case is mediated by HONO via facile H-exchange involving a seven-centered transition state analogous to **LM4**. Practically, the formation of H_3NO and H_2NOH is irrelevant and inconsequential to the chemistry of the $NH_3 + HNO_3$ reaction.

As mentioned above, the bimolecular reactions 1 and 2 of NH_3 with HNO_3 producing the two isomeric products H_2NNO_2 and H_2NONO, respectively, are controlled entirely by the rates of their passage over **TS1** and **TS2**, respectively. By means of the energy barriers calculated and summarized in Table 1 and molecular parameters as well as frequencies presented in Table 4 for the reactants and TSs, TST calculations with tunneling corrections gave rise to the following expressions for their rate constants [in units of $cm^3/(mol·s)$] covering the 300−1000 K temperature range:

$$k_1 = 8.42 \times 10^{11} e^{-23440/T}$$

$$k_2 = 3.09 \times 10^{12} e^{-24390/T}$$

The tunneling correction for reaction 1 amounts to about 48% at 500 K and 12% at 1000 K; the correction for reaction 2 is, however, negligible (<1%) because of its low imaginary frequency. For a broader temperature of 300−3000 K, they can be effectively presented by the following three-parameter forms:

$$k_1 = 0.81 T^{3.47} e^{-21670/T}$$

$$k_2 = 23.2 T^{3.50} e^{-22610/T}$$

These rate constants are recommended for kinetic modeling of AN and ADN.

IV. Conclusion

The results of our ab initio MO calculations employing the G2M method reveal the possibility of a nonionic bimolecular reaction taking place between NH_3 and HNO_3. The reaction was found to occur by two distinct transition states producing H_2O and two reactive isomeric molecular intermediates, H_2NNO_2 and H_2NONO, with a similar reaction barrier, 46 kcal/mol. The former, formed by a tighter four-centered transition state, is predicted to be a minor product, although it is energetically more stable than the latter, formed by a looser five-centered transition state. The rate constants for these two processes have been calculated with the transition-state theory; they are recommended for the kinetic modeling of AN and ADN combustion reactions.

Acknowledgment. This work was sponsored partly by Emory University and partly by the Caltech Multidisciplinary University Research Initiative under ONR Grant No. N00014-95-1-1388, Program Manager Dr. Richard S. Miller. Also, we are thankful to the Cherry L. Emerson Center for Scientific Computation for the use of various programs and computing facilities.

References and Notes

(1) Greenwood, N. N.; Earnshaw, A. *Chemistry of Elements*; Pergamon Press: Oxford, 1984; p 541.
(2) Cotton, F. A.; Wilkinson, G. *Adv. Inorg. Chem*., 5th ed.; John Wiley: New York, 1988.
(3) Diau, E. W. G.; Lin, M. C.; He, Y.; Melius, C. F. *Prog. Energy Combust. Sci*. **1995**, *21*, 1.
(4) Diau, E. W. G.; Halbgewachs, M. J.; Smith, A. R.; Lin, M. C. *Int. J. Chem. Kinet*. **1995**, *27*, 867.
(5) Mebel, A. M.; Morokuma, K.; Lin, M. C.; Melius, C. F. *J. Phys. Chem*. **1995**, *99*, 1900.
(6) Mebel, A. M.; Morokuma, K.; Lin, M. C. *J. Chem. Phys*. **1994**, *101*, 3916.
(7) Mebel, A. M.; Hsu, C.-C.; Lin, M. C.; Morokuma, K. *J. Chem. Phys*. **1995**, *103*, 5640.
(8) Diau, E. W. G.; Yu, T.; Wagner, M. A. G. Lin, M. C. *J. Phys. Chem*. **1994**, *98*, 4034.
(9) Mebel, A. M.; Lin, M. C.; Morokuma, K.; Melius, C. F. *Int. J. Chem. Kinet*. **1996**, *28*, 693.
(10) Mebel, A. M.; Lin, M. C.; Morokuma, K.; Melius, C. F. *J. Phys. Chem*. **1995**, *99*, 6842.
(11) Mebel, A. M.; Diau, E. W. G.; Lin, M. C.; Morokuma, K. *J. Phys. Chem*. **1996**, *100*, 7517.
(12) Halbgewachs, M. J.; Diau, E. W. G.; Mebel, A. M.; Lin, M. C.; Melius, C. F. *Proceedings of the 26th International Symposium on Combustion;* The Combustion Institute: Pittsburgh, PA, 1996; p 2109.
(13) Hsu, C.-C.; Lin, M. C.; Mebel, A. M.; Melius, C. F. *J. Phys. Chem. A* **1997**, *101*, 60.
(14) Boughton, J. W.; Kristyan, S.; Lin, M. C. *Chem. Phys*. **1997**, *214*, 219.
(15) Park, J.; Lin, M. C. *J. Phys. Chem*. **1997**, *A101*, 5.
(16) Park, J.; Lin, M. C. *J. Phys. Chem*. **1997**, *A101*, 2643.
(17) Mebel, A. M.; Lin, M. C.; Morokuma, K. *Int. J. Chem. Kinet*., submitted.
(18) Park., J.; Lin, M. C. Unpublished work.
(19) (a) Pople, J. A.; Head-Gordon, M.; Fox, D. J.; Raghavachari, K.; Curtiss, L. A. *J. Chem. Phys*. **1989**, *90*, 5622. (b) Curtiss, L. A.; Jones, C.; Trucks, G. W.; Raghavachari, K.; Pople, J. A. *J. Chem. Phys*. **1990**, *93*, 2537. (c) Curtiss, L. A.; Raghavachari, K.; Trucks, G. W.; Pople, J. A. *J. Chem. Phys*. **1991**, *94*, 7221
(20) Madden, L.; Moskaleva, L. V.; Kristyan, S.; Lin, M. C. *J. Phys. Chem. A* **1997**, *101*, 6790.
(21) Park, J.; Dyakov, I. V.; Mebel, A. M.; Lin, M. C. *J. Phys. Chem. A* **1997**, *101*, 6043.
(22) Hehre, W.; Radom, L.; Schleyer, P. v. R.; Pople, J. A. *Ab Initio Molecular Orbital Theory*; Wiley: New York, 1986.

(23) (a) Purvis, G. D.; Bartlett, R. J. *J. Chem. Phys.* **1982**, *76*, 1910. (b) Hampel, C.; Peterson, K. A.; Werner, H.-J. *Chem. Phys. Lett.* **1992**, *190*, 1. (c) Knowles, P. J.; Hampel, C.; Werner, H.-J. *J. Chem. Phys.* **1994**, *99*, 5219. (d) Deegan, M. J. O.; Knowles, P. J. *Chem. Phys. Lett.* **1994**, *227*, 321.

(24) (a) Becke, A. D. *J. Chem. Phys.* **1993**, *98*, 5648; (b) **1992**, *96*, 2155; (c) **1992**, *97*, 9173.

(25) Lee, C.; Yang, W.; Parr, R. G. *Phys. Rev.* **1988**, *B37*, 785.

(26) Gonzalez, C.; Schlegel, H. B. *J. Chem. Phys.* **1989**, *90*, 2154.

(27) Frisch, M. J.; Trucks, G. W.; Schlegel, H. B.; Gill, P. M. W.; Johnson, B. G.; Robb, M. A.; Cheeseman, J. R.; Keith, T.; Petersson, G. A.; Montgomery, J. A.; Raghavachari, K.; Al-Laham, M. A.; Zakrzewski, V. G.; Ortiz, J. V.; Foresman, J. B.; Cioslowski, J.; Stefanov, B. B.; Nanayakkara, A.; Challacombe, M.; Peng, C. Y.; Ayala, P. Y.; Chen, W.; Wong, M. W.; Andres, J. L.; DeFrees, D. J.; Baker, J.; Stewart, J. P.; Head-Gordon, M.; Gonzalez, C.; Pople, J. A. *GAUSSIAN 94*, Revision D. 3; Gaussian, Inc., Pittsburgh, PA, 1995.

(28) Melius, C. F. In *Chemistry and Physics of Energetic Materials*; Bulusu, S., Ed; Nato ASI 309; 1990; p 21.

(29) Saxon, R. P.; Yoshimine, M. *J. Phys. Chem.* **1989**, *93*, 3130.

(30) Sadova, N. I.; Slepnev, G. E.; Tarasenko, N. A.; Zenkin, A. A.; Vilkov, L. V.; Shishkov, I. F.; Pankrushev, Yu. A. *Zh. Strukt. Klim.* **1997**, *18*, 865.

(31) Luckhaus, D. *Ber. Bunsen-Ges. Phys. Chem.* **1997**, *101*, 346.

(32) Bach, R. D.; Owensby, A. L.; Gonzalez, C.; Schlegel, H. B.; McDouall, J. J. W. *J. Am. Chem. Soc.* **1991**, *113*, 6001.

(33) Trindle, C.; Shillady, D. D. *J. Am. Chem. Soc.* **1973**, *95*, 703.

(34) Wallmeier, H.; Kutzelnigg, W. *J. Am. Chem. Soc.* **1979**, *101*, 2804.